

2022-09-14

A novel tool for quantitative measurement of distortion in keratoconus

Joshi, Mahesh Raj

<http://hdl.handle.net/10026.1/19897>

10.1038/s41433-022-02240-x

Eye

Springer Science and Business Media LLC

All content in PEARL is protected by copyright law. Author manuscripts are made available in accordance with publisher policies. Please cite only the published version using the details provided on the item record or document. In the absence of an open licence (e.g. Creative Commons), permissions for further reuse of content should be sought from the publisher or author.

1 **A novel tool for quantitative measurement of distortion in keratoconus**

2 **Mahesh R Joshi¹, Kenrick J Voison², Marianne Coleman³, Niall Farnon², Peter Bex⁴**

3 **Affiliations:** ¹ Eye and Vision Research Group, School of Health Professions, University of Plymouth,
4 Plymouth, United Kingdom

5 ² Optometry Unit, Faculty of Health, St. Augustine Campus, The University of the West Indies, St. Augustine,
6 Trinidad & Tobago

7 ³ Department of Optometry and Vision Sciences, University of Melbourne, Victoria, Australia

8 ⁴ Psychology Department, Northeastern University, Boston, USA

9

10 **Corresponding author:** Mahesh R Joshi; Mahesh.Joshi@plymouth.ac.uk

11

12 **Abstract**

13 **Background:** Keratoconus is associated with thinning and anterior protrusion of the cornea resulting
14 in the symptoms of blurry and distorted vision. The commonly used clinical vision tests such as visual
15 acuity and contrast sensitivity may not reflect the symptoms experienced in keratoconus and there are
16 no quantitative tools to measure visual distortion. In this study, we used a quantitative test based on
17 vernier alignment and field matching techniques to quantify visual distortion in keratoconus and
18 assess its relation to corneal structural changes.

19 **Methods:** A total of 50 participants (25 keratoconus and 25 visually normal) completed the
20 experiment where they aligned supra-threshold white target circles in opposite field in reference to
21 guide lines and circles to complete a square structure. The task was repeated five times and the global
22 distortion index (GDI) and global uncertainty index (GUI) were calculated as the mean and standard
23 deviation respectively of local perceived misalignment of target circles over five trials.

24 **Results:** Both GDI and GUI were higher in participants with keratoconus compared to controls ($p <$
25 0.01). Both parameters correlated with the best corrected visual acuity, maximum corneal curvature
26 (K_{max}), topographical keratoconus classification (TKC) and central corneal thickness (CCT).

27 **Conclusion:** Our findings show that the quantitative measure of distortion could be a useful tool for
28 behavioural assessment of progressive keratoconus.

29 **Introduction**

30 Keratoconus is a progressive corneal condition characterised by anterior protrusion and thinning of
31 the cornea. The aetiology of the condition is multifactorial with recent studies suggesting a role of
32 inflammatory mechanisms.(1, 2) The estimated prevalence of keratoconus is reported to be 1 in 84
33 (3) to 1 in 375 (4) in young adults. The condition has a genetic heterogeneity and involves both
34 autosomal dominant and autosomal recessive patterns.(5) The corneal structural changes lead to
35 irregular astigmatism and myopia with the symptoms of blurry vision, increased sensitivity to glare,
36 and distorted vision due to higher order aberrations.(6-8) The symptoms begin in adolescence or early
37 adulthood and usually slowly progresses until mid-adulthood.(8)

38

39 The commonly assessed structural measurements in keratoconus include corneal curvature, corneal
40 topography, and corneal thickness using keratometer, corneal topographer, and ocular coherence
41 tomogram (OCT) respectively. Visual acuity is the most commonly measured visual function
42 outcome in the clinical setup. However, visual acuity is not a good predictor of symptoms experienced
43 in keratoconus and vision related quality of life is reduced even in early stages of the disorder while
44 good visual acuity may be maintained. (9-12) Contrast sensitivity meanwhile correlates both with
45 higher order aberration (7, 13) and topographic indices (14). However, clinically available contrast
46 sensitivity charts may not be appropriate for the evaluation of moderate to advanced keratoconus. (15)
47 Hence there is a lack of a perceptual visual measure that reflects symptoms experienced in
48 keratoconus. Different parameters indicate keratoconus progression, and therefore need for
49 intervention with methods such as collagen cross-linking. These include an increase in maximum
50 corneal curvature by 1 D over a year (16), increase in astigmatism by 1 - 3 DC over 6 months, and
51 reduction in central corneal thickness by 5% over 6 months (17). Previous studies have demonstrated
52 variable correlation of best-corrected visual acuity with these parameters, with contrast sensitivity
53 again showing a better correlation.(18, 19) However, monitoring clinical progression requires
54 specialist imaging equipment, and therefore regular visits to an eye care professional are required.
55 Recently a new scoring system that includes clinical measures and the patient characteristics such as
56 patient reported quality of vision, the Dutch Crosslinking for Keratoconus Score, is reported to be

57 better at predicting when medical intervention may be needed.(20) A reliable perceptual
58 measurement that better reflects patient's visual status may further aid development of such scoring
59 system. Such a measure could also potentially be used as a home-based test.

60

61 While visual distortion is one of the most common symptoms in keratoconus, there are currently
62 limited methods to quantify such distortion and none as far as we are aware specifically designed for
63 keratoconus. There have been approaches to quantify distortion using hyperacuity tasks in different
64 ocular conditions. (21-24) Hyperacuity refers to the visual system's ability to perform spatial tasks
65 beyond the eye's classical resolution limit with thresholds as low as 3 to 6 secs of arc. (25, 26) Vernier
66 alignment (vernier acuity), a classic hyperacuity task where participants discriminate difference in the
67 relative spatial localisation of two or more visual stimuli such as lines or dots has been used in
68 previous studies (27-29). The use of such methods for conditions such as amblyopia (30) and age-
69 related macular degeneration (AMD) (31) have demonstrated perceptual distortions exhibit a similar
70 dissociation from visual acuity as clinical keratoconus indices. Thus, evaluating perceptual distortions
71 may provide a more nuanced characterisation of visual function for ocular diseases.

72

73 In this study, we used a quantitative paradigm based on both vernier alignment and field matching
74 techniques to quantify visual distortion experienced in keratoconus and assess its relation to corneal
75 structural changes. Providing a means to reliably and systematically characterise the visual deficit in
76 keratoconus enables future studies exploring the impact of established treatments upon these deficits.

77

78 **Methods**

79 **Participants:**

80 A total of 25 participants (mean age = 29.84 ± 7.46 years, 15 females) with keratoconus at different
81 disease stages and 25 normal controls (mean age = 22.12 ± 2.62 years, 17 females) were recruited for
82 the study. All participants underwent measurements of the best-corrected monocular visual acuity
83 (BCVA) with Bailey-Lovie log MAR chart after refraction with autorefractor (Topcon KR-8000PA)

84 by an optometrist. The corneal assessment to ascertain keratoconus signs was carried out using
 85 Haag-Streit slit-lamp biomicroscope. The corneal mapping was conducted using a corneal
 86 topographer (Oculus Keratograph D-35582) and the central corneal thickness (CCT) was measured
 87 using anterior segment ocular coherence tomogram (Topcon 3D OCT-2000). A specialist
 88 established the keratoconus diagnosis based on the maximum corneal curvature (K_{max}) of $\geq 50.00Ds$
 89 with topographic keratoconus classification (TKC) grading of >1.0 and the presence of classical
 90 keratoconus sign in either eye. The signs considered were Munson's sign, Rizutii's sign, Vogt striae,
 91 and Fleischer ring, in addition to scissors reflex on retinoscopy. The clinical details of the keratoconus
 92 and control group are presented in Table 1.

93

94 Table 1: Clinical attributes of keratoconus and control participants

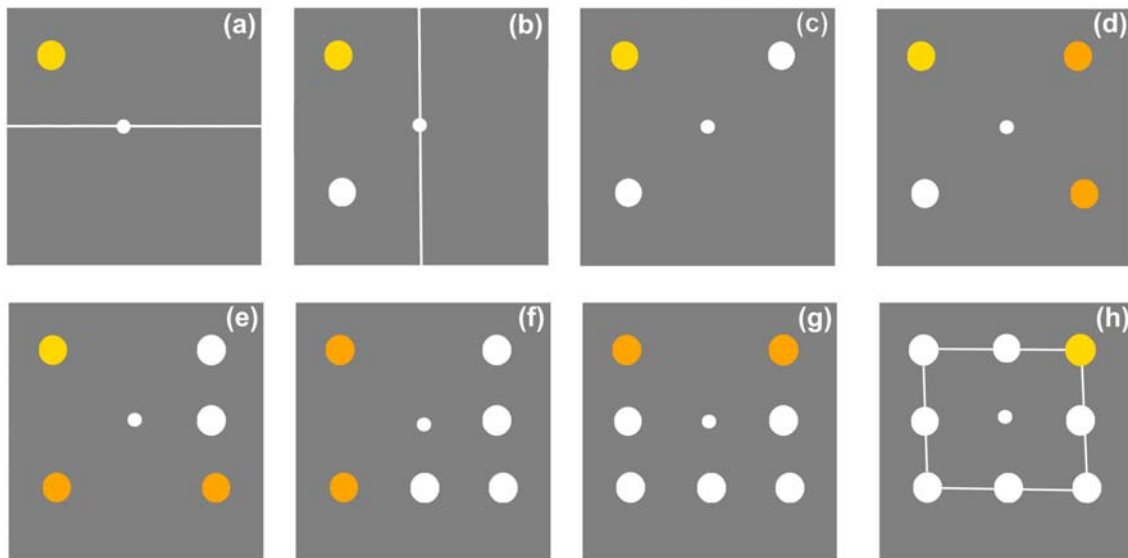
Clinical parameters	Keratoconus ($n = 50$ eyes)	Control ($n = 50$ eyes)
Best-corrected visual acuity, log MAR, mean (SD), mean	0.21 (0.27), 6/9.6	-0.09 (0.06), 6/4.8
Snellen		
Refractive error (Sphere), diopter cylinder, mean (SD)	- 2.52 (2.85)	- 1.14 (1.61)
Refractive error (Cylindrical), diopter cylinder, mean (SD)	-3.45 (2.10)	-0.77 (0.90)
Maximum corneal curvature, dioptre, mean (SD)	54.48 (6.09)	45.66 (1.58)
Mean corneal curvature, dioptre, mean (SD)	47.03 (3.96)	44.51 (1.41)
Central corneal thickness, micrometre (μm), mean (SD)	495.34 (47.50)	554.36 (25.71)

95

96 **Stimuli and procedure**

97 The experimental stimulus was created and presented using MATLAB (32) software with
 98 psychtoolbox extensions (Psychtoolbox 3.0) (33, 34) and presented on a computer screen with the
 99 resolution of 1920 x 1080 pixels. The task combined vernier alignment and field matching techniques.
 100 The stimuli consisted of eight circles (suprathreshold acuity and contrast) each subtending 0.37° at the
 101 viewing distance of 90cm. The task for the observer was to align target circles with computer mouse
 102 click in relation to a reference line and circles presented against a 75% contrast grey background
 103 monocularly. At the start of the experiment a white central fixation circle (0.14°) and a white
 104 horizontal line were presented. This was followed by the presentation of a yellow reference circle

105 (0.37°) at the eccentricity of 0.73° from the central fixation (Figure 1; a). The task for the participant
 106 was to align a white target circle with the yellow reference circle at an equal distance from the
 107 horizontal reference line (Figure 1; a & b). After the placement of the first circle, the reference line
 108 was presented vertically, and the participant aligned the next target circle in the opposite field (Figure
 109 1; b & c). Following this, the reference line was removed, and the participant placed another target
 110 circle to complete the remaining corner of a "virtual square" (Figure 1, d). Following this, two dots
 111 changed colour to orange (reference dots) and the task for the participant was to place the target
 112 circles at the mid-point and in alignment with these reference dots (Figure 1, e - g). The process
 113 continued until a square shape was completed by placing a total of seven target circles. (Figure 1, h).
 114 Participants fixated on a central target (0.14°) throughout the task. There was no time limit for the
 115 completion of the task. If the participant reported having made an error with the dot placement (e.g.
 116 mis-click), the researcher removed the dot to allow another attempt.



117

118 **Figure 1: Schematic representation of the experimental task. The task was to position a supra-threshold contrast**
 119 **white circle in relation to the white line and/or yellow/orange circles to complete a square shape (bottom right panel).**

120 a) Starting view for the participant (starting corner is randomised). Participant aligns a white dot (shown in b) with yellow
 121 dot on the opposite side of the white line to match the reference space.

122 b) Repeat of a) using vertical reference line and horizontal reference space.

123 c - d) Complete the square by aligning the remaining dots horizontally and vertically.

124 e) Fill in the space between the two orange dots in alignment with the central fixation target.

125 f - g) Repeat step e) on each side to finish reconstructing the square.

126 h) Final image shown to the participant after all clicks are completed.

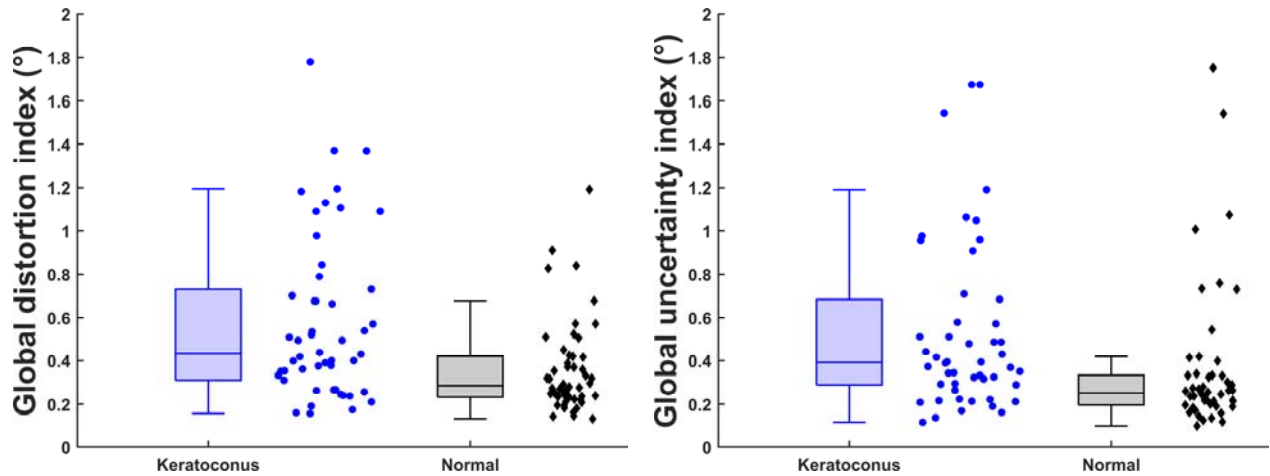
127 Written informed consent was obtained from all participants once the nature of the experiment was
128 explained. The experiment was completed monocularly with the patient's best correction in place in a
129 dark room, with the computer monitor being the only light source. The distance from the monitor was
130 controlled using head and chin rest. The task was repeated five times and the global distortion index
131 (GDI) and global uncertainty index (GUI) were calculated as the mean and standard deviation
132 respectively of local perceived misalignment of target circles over five trials. (30) The distortion data
133 for both keratoconus and normal controls did not follow a normal distribution (Shapiro-Wilk test, $p <$
134 0.001) hence nonparametric statistics were used for all analyses. The study followed the tenets of
135 Helsinki declaration on human research participants and the research protocol was approved by the
136 Campus Research Ethics Committee of the Faculty of Health, St. Augustine campus, the University of
137 the West Indies.

138

139 **Results**

140 The visual distortion measured as the global distortion index (GDI) was higher in keratoconus eyes (n
141 $= 50$, median (M) $= 0.43^\circ$) compared to the control eyes ($n = 50$, $M = 0.29^\circ$), Mann-Whitney $U = 756$,
142 $z = -3.41$, $p = 0.001$. Similarly, the global uncertainty index (GUI) was also higher in keratoconus
143 eyes ($n = 50$, $M = 0.39^\circ$) compared to the control eyes ($n = 50$, $M = 0.25^\circ$), Mann-Whitney $U = 763$, z
144 $= -3.36$, $p = 0.001$. (Figure 2)

145



146

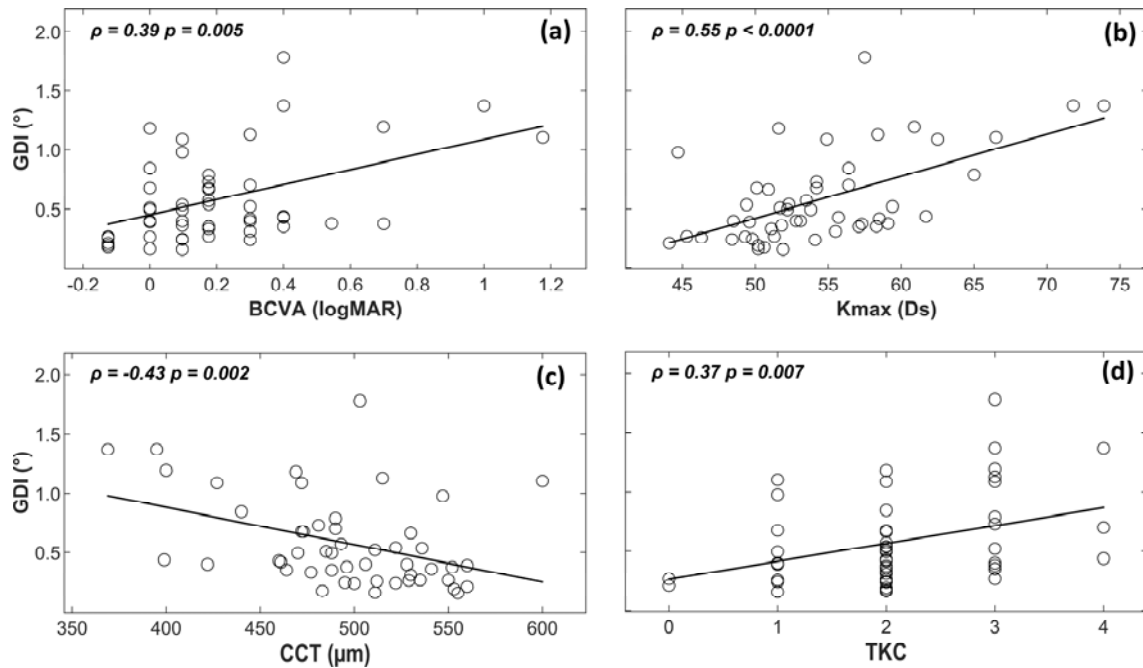
147 **Figure 2: Boxplots comparing global distortion index (left panel) and global uncertainty index (right panel) between**
 148 **keratoconus eyes ($n = 50$) and normal eyes ($n = 50$). Box bounds: upper/lower quartile; horizontal bar within box**
 149 **bounds: median. All data points are also presented.**

150

151 The relation between clinical parameters and distortion indices (GDI and GUI) were investigated
 152 using Spearman's rank order correlation. These are shown for GDI in Figure 3 and GUI in Figure 4
 153 for BCVA (Figure 3a, 4a), maximum corneal curvature (Figure 3b, 4b), central corneal thickness
 154 (Figure 3c, 4c) and topographic keratoconus classification (TKC) scores (Figure 3d, 4d). Among the
 155 clinical parameters, BCVA strongly correlated with maximum corneal curvature (Spearman's ρ ($\rho = 0.73, p < 0.001$)) and moderately correlated with TKC scores ($\rho = 0.49, p < 0.001$) but not with
 156 central corneal thickness ($\rho = -0.27, p = 0.06$). Thus, poorer BCVA was associated with greater
 157 maximum corneal curvature and TKC scores.

159

160 For the distortion indices, GDI was weakly correlated with BCVA ($\rho = 0.39, p = 0.005$, Figure 3a),
 161 moderately correlated with maximum corneal curvature ($\rho = 0.55, p < 0.001$, Figure 3b) and weakly
 162 correlated with TKC scores ($\rho = 0.32, p = 0.02$, Figure 3d). A moderate negative correlation was also
 163 observed between GDI and central corneal thickness ($\rho = -0.43, p = 0.002$, Figure 3c). Thus, higher
 164 GDI was associated with poorer BCVA, greater maximum corneal curvature and TKC scores, and
 165 lower central corneal thickness.



166

167

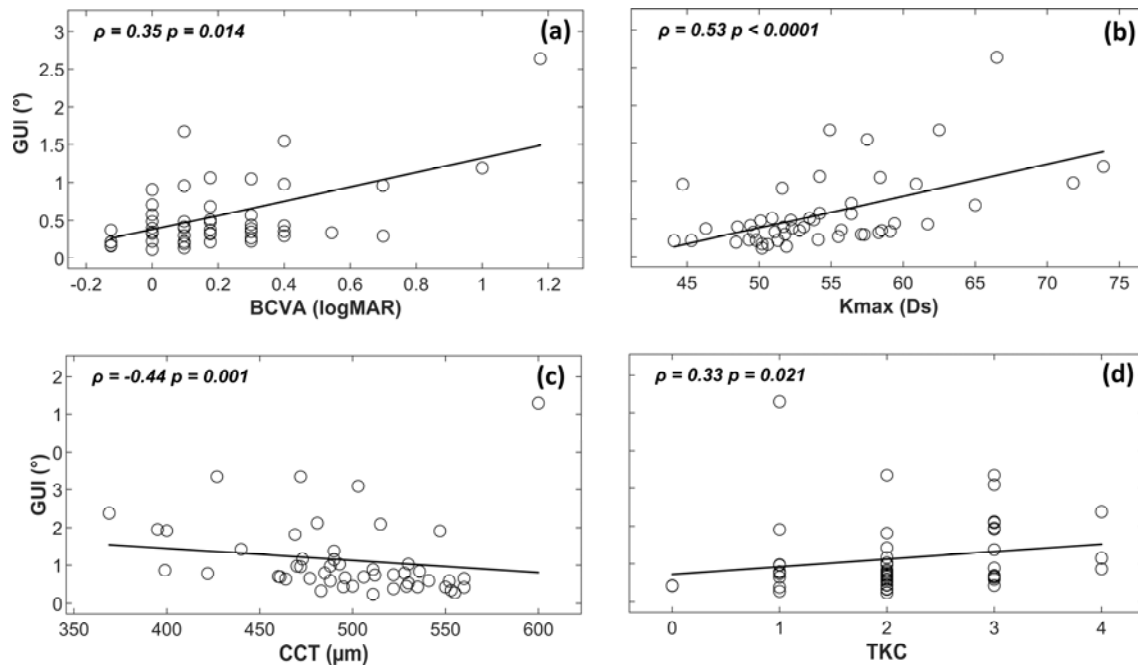
168 **Figure 3: The scatterplots showing correlation between global distortion index (GDI) with a) the best corrected visual**
 169 **acuity (BCVA), b) maximum corneal curvature (K_{max}), c) central corneal thickness (CCT), and d) topographic**
 170 **keratoconus classification (TKC). The red line represents least square regression line. The Spearman's rho (ρ) and**
 171 **the p value are also provided.**

172

173 The global uncertainty index (GUI) also exhibited a weak positive correlation with BCVA ($\rho = 0.35$,
 174 $p = 0.01$, Figure 4a), moderate correlation with maximum corneal curvature ($\rho = 0.53$, $p < 0.001$,
 175 Figure 4b) and weak correlation with TKC scores ($\rho = 0.32$, $p = 0.02$, Figure 4d). A moderate
 176 negative correlation was also observed between the GUI and the central corneal thickness (CCT) ($\rho =$
 177 -0.44 , $p = 0.001$, Figure 4c). Thus, higher GUI was associated with poorer BCVA, greater maximum
 178 corneal curvature and TKC scores, and lower central corneal thickness.

179

180



181

182

183

Figure 4: The scatterplots showing correlation between global uncertainty index (GUI) with a) the best-corrected visual acuity (BCVA), b) maximum corneal curvature (K_{max}), c) central corneal thickness (CCT), and d) topographic keratoconus classification (TKC). The red line represents least square regression line. The Spearman's rho (ρ) and the p value are also provided.

187

188 Discussion

189 This study for the first time quantitatively evaluated visual distortion experienced in keratoconus. The
 190 results showed that visual distortion was higher in individuals with keratoconus compared to the
 191 normally sighted controls. The distortion indices also correlated with commonly measured clinical
 192 metrics of keratoconus such as K_{max} and TKC.

193

194 The results demonstrate that measurements of visual distortion obtained with our paradigm
 195 differentiate individuals with keratoconus from those without. A similar paradigm based on vernier
 196 alignment has been used to measure perceptual distortion in amblyopia and AMD before. (30, 31, 35,
 197 36) However these tests are lengthy to conduct in a clinical setting compared to the combined vernier
 198 alignment and field matching task used in the current study, which takes just a few minutes to

199 complete. This renders our paradigm a more viable option for characterising visual distortions
200 associated with keratoconus in clinical settings.
201

202 Both GDI and GUI increased with worsening visual acuity, albeit the correlation was weak. Using
203 similar methods of distortion quantification, distortions were found to be higher in the amblyopic
204 population compared to non-amblyopic controls. (30, 35) Amblyopic observers experience chronic
205 distortion during development and may learn the spatial form of distorted optotypes. In contrast,
206 AMD patients have an acquired deficit later in life and visual distortion (metamorphopsia) arises at
207 the retinal level. Although research concerning the underlying basis of metamorphopsia in these
208 patient groups continues to be limited, it has been suggested that the visual processing stream in such
209 instances may be subject to top-down influences as a result of the slow progressing nature of the
210 aetiologies, potentially resulting in some degree of visual adaptation to the degraded image quality
211 and a resulting dissociation of perceived metamorphopsia from the visual acuity deficit. (31) Such
212 influences may also explain why we found a higher GUI (index of stability of the visual percept) that
213 correlated with certain clinical keratoconus indices.
214

215 In our sample, poorer BCVA was associated with greater maximum corneal curvature ($\rho = 0.73$) and
216 TKC scores ($\rho = 0.49$) but was not significantly correlated with CCT ($\rho = -0.27$). Previous studies
217 have shown that visual acuity shows a variable degree of correlation with the corneal structural
218 measures and vision related quality of life in keratoconus. (9-11, 37) In comparison, contrast
219 sensitivity has been found to correlate with corneal irregularities (37), higher order aberrations (13),
220 and vision related quality of life (12). However, proper measurement of contrast sensitivity is time
221 consuming and traditional clinical tests of contrast sensitivity such as VisTech chart have limited
222 spatial frequencies for evaluation of moderate to advanced keratoconus. (15) Hence, the distortion
223 test used in the current study could provide an alternative or adjunctive visual measure for
224 keratoconus.
225

226 The visual distortion indices also correlated with commonly measured corneal structural parameters.
227 Both GDI and GUI increased with higher corneal curvature, higher TKC and lower corneal thickness.
228 The maximum corneal curvature (K_{\max}) and central corneal thickness better reflect the quality of life
229 measures in keratoconus compared to visual acuity. (38, 39) Distortion measurement could therefore
230 serve as a helpful bridge between clinical indicators and perceived quality of life that is quick and
231 simple to administer.

232

233 In recent times home monitoring of different ocular conditions have been used (31, 40, 41) and these
234 have become even more important due to the COVID-19 pandemic, during which it has been
235 necessary in many instances to constrain in-person clinical interactions to essential care. Various
236 home-based applications implemented on the digital devices show good reliability compared to the
237 hospital-based tests for different ocular conditions. (40-44) As far as we are aware, there are no
238 systematic measures of distortion in keratoconus that could be utilised in this context. Proper
239 monitoring in keratoconus could ensure timely medical intervention such as collagen crosslinking but
240 requires assessment by an eye care professional using specialist imaging equipment. A simple
241 monocular visual task such as that used in the current study could be easily transformed into a home-
242 based tool. This also holds promise for individuals living with keratoconus in remote or rural areas
243 with limited specialist access. In future, we will develop a version of the distortion test for use on
244 personal or portable computing devices, to explore the use of the test as a home based tool for
245 keratoconus.

246

247 Some limitations can be identified for our study. Firstly, our paradigm provides information about
248 distortion magnitude, but less about the individual's subjective percept, e.g. magnification, barrel
249 distortion, etc. If clinically relevant, practitioners can store the square drawings to retain as a way of
250 visually monitoring distortion over time. However, at present we are not able to offer a systematic
251 method for detecting significant changes in the shape of the constructed square, which has the
252 capacity to change significantly while yielding similar GDI and GUI measurements. This could be
253 developed in future using image processing techniques or through methods such as subdivision into

254 quadrant-based GDI and GUI measurements. Additionally, the value of a measurement tool to detect
255 progression of keratoconus remediation following treatment will depend on the repeatability of
256 distortion measurements, which is the focus of future work. Secondly, this was a cross-sectional
257 study and we are unable to provide information about the extent to which treatments for keratoconus
258 such as cross-linking may affect such measurements. As the correlation between BCVA and our
259 distortion measures was modest, we cannot be certain whether interventions to improve visual acuity
260 will impact GDI and GUI. As such, whether these distortion measures could be used to support
261 clinical decision-making about keratoconus interventions or as a treatment outcome measure should
262 be a focus of future work.

263

264 **References**

265

- 266 1. Loh IP, Sherwin T. Is Keratoconus an Inflammatory Disease? The Implication of Inflammatory
267 Pathways. *Ocular Immunology and Inflammation*. 2022;30(1):246-55.
- 268 2. Wisse RP, Kuiper JJ, Gans R, Imhof S, Radstake TR, Van der Lelij A. Cytokine Expression in
269 Keratoconus and its Corneal Microenvironment: A Systematic Review. *Ocul Surf*. 2015;13(4):272-83.
- 270 3. Chan E, Chong EW, Lingham G, Stevenson LJ, Sanfilippo PG, Hewitt AW, et al. Prevalence of
271 Keratoconus Based on Scheimpflug Imaging: The Raine Study. *Ophthalmology*. 2021;128(4):515-21.
- 272 4. Godefrooij DA, de Wit GA, Uiterwaal CS, Imhof SM, Wisse RP. Age-specific Incidence and
273 Prevalence of Keratoconus: A Nationwide Registration Study. *Am J Ophthalmol*. 2017;175:169-72.
- 274 5. Edwards M, McGhee CNJ, Dean S. The genetics of keratoconus. *Clinical & Experimental*
275 *Ophthalmology*. 2001;29(6):345-51.
- 276 6. Applegate RA, Hilmantel G, Howland HC, Tu EY, Starck T, Zayac EJ. Corneal first surface
277 optical aberrations and visual performance. *Journal of refractive surgery (Thorofare, NJ : 1995)*.
278 2000;16(5):507-14.
- 279 7. Okamoto C, Okamoto F, Samejima T, Miyata K, Oshika T. Higher-order wavefront aberration
280 and letter-contrast sensitivity in keratoconus. *Eye*. 2008;22(12):1488-92.
- 281 8. Rabinowitz YS. Keratoconus. *Survey of Ophthalmology*. 1998;42(4):297-319.
- 282 9. Steinberg J, Bußmann N, Frings A, Katz T, Druchkiv V, Linke SJ. Quality of life in stable and
283 progressive 'early-stage' keratoconus patients. *Acta Ophthalmologica*. 2020;n/a(n/a).
- 284 10. Kymes SM, Walline JJ, Zadnik K, Gordon MO. Quality of life in keratoconus. *American Journal*
285 *of Ophthalmology*. 2004;138(4):527-35.
- 286 11. Sahebzada S, Fenwick EK, Xie J, Snibson GR, Daniell MD, Baird PN. Impact of Keratoconus in
287 the Better Eye and the Worse Eye on Vision-Related Quality of Life. *Invest Ophthalmol Vis Sci*.
288 2014;55(1):412-6.
- 289 12. Kandel H, Pesudovs K, Watson SL. Measurement of Quality of Life in Keratoconus. *Cornea*.
290 2020;39(3).
- 291 13. Shneor E, Piñero DP, Doron R. Contrast sensitivity and higher-order aberrations in
292 Keratoconus subjects. *Scientific Reports*. 2021;11(1):12971.

293 14. Maeda N, Sato S, Watanabe H, Inoue Y, Fujikado T, Shimomura Y, et al. Prediction of letter
294 contrast sensitivity using videokeratographic indices. *American Journal of Ophthalmology*.
295 2000;129(6):759-63.

296 15. Zadnik K, Mannis MJ, Johnson CA, Rich D. Rapid contrast sensitivity assessment in
297 keratoconus. *Am J Optom Physiol Opt*. 1987;64(9):693-7.

298 16. Raiskup-Wolf F, Hoyer A, Spoerl E, Pillunat LE. Collagen crosslinking with riboflavin and
299 ultraviolet-A light in keratoconus: Long-term results. *Journal of Cataract & Refractive Surgery*.
300 2008;34(5):796-801.

301 17. Vinciguerra P, Albè E, Trazza S, Rosetta P, Vinciguerra R, Seiler T, et al. Refractive,
302 Topographic, Tomographic, and Aberrometric Analysis of Keratoconic Eyes Undergoing Corneal
303 Cross-Linking. *Ophthalmology*. 2009;116(3):369-78.

304 18. Pérez-Rueda A, Castro-Luna G. A model of visual limitation in patients with keratoconus.
305 *Scientific Reports*. 2020;10(1):19335.

306 19. Esaka Y, Kojima T, Dogru M, Hasegawa A, Tamaoki A, Uno Y, et al. Prediction of Best-
307 Corrected Visual Acuity With Swept-Source Optical Coherence Tomography Parameters in
308 Keratoconus. *Cornea*. 2019;38(9):1154-60.

309 20. Wisse RPL, Simons RWP, van der Vossen MJB, Muijzer MB, Soeters N, Nuijts RMMA, et al.
310 Clinical Evaluation and Validation of the Dutch Crosslinking for Keratoconus Score. *JAMA*
311 *Ophthalmology*. 2019;137(6):610-6.

312 21. Goldstein M, Loewenstein A, Barak A, Pollack A, Bukelman A, Katz H, et al. Results of a
313 multicenter clinical trial to evaluate the preferential hyperacuity perimeter for detection of age-
314 related macular degeneration. *Retina*. 2005;25(3):296-303.

315 22. Pitrelli Vazquez N, Knox PC. Assessment of visual distortions in age-related macular
316 degeneration: emergence of new approaches. *Br Ir Orthopt J*. 2015;12:9-15.

317 23. Pitrelli Vazquez N, Harding SP, Heimann H, Czanner G, Knox PC. Radial shape discrimination
318 testing for new-onset neovascular age-related macular degeneration in at-risk eyes. *PLoS One*.
319 2018;13(11):e0207342-e.

320 24. Wang Y-Z, Wilson E, Locke KG, Edwards AO. Shape Discrimination in Age-Related Macular
321 Degeneration. *Invest Ophthalmol Vis Sci*. 2002;43(6):2055-62.

322 25. Westheimer G. Visual acuity and hyperacuity: resolution, localization, form. *Am J Optom*
323 *Physiol Opt*. 1987;64(8):567-74.

324 26. Westheimer G. The spatial sense of the eye. Proctor lecture. *Invest Ophthalmol Vis Sci*.
325 1979;18(9):893-912.

326 27. Fang MS, Enoch JM, Lakshminarayanan V, Kim E, Kono M, Strada E, et al. The three point
327 vernier alignment or acuity test (3Pt VA test): an analysis of variance. *Ophthalmic & physiological*
328 *optics : the journal of the British College of Ophthalmic Opticians (Optometrists)*. 2000;20(3):220-34.

329 28. McKendrick AM, Johnson CA, Anderson AJ, Fortune B. Elevated Vernier Acuity Thresholds in
330 Glaucoma. *Invest Ophthalmol Vis Sci*. 2002;43(5):1393-9.

331 29. Little J-A, Woodhouse JM, Lauritzen JS, Saunders KJ. Vernier Acuity in Down Syndrome.
332 *Invest Ophthalmol Vis Sci*. 2009;50(2):567-72.

333 30. Piano MEF, Bex PJ, Simmers AJ. Perceptual Visual Distortions in Adult Amblyopia and Their
334 Relationship to Clinical Features. *Invest Ophthalmol Vis Sci*. 2015;56(9):5533-42.

335 31. Wiecek E, Lashkari K, Dakin SC, Bex P. Novel Quantitative Assessment of Metamorphopsia in
336 Maculopathy. *Invest Ophthalmol Vis Sci*. 2015;56(1):494-504.

337 32. MATLAB. 8.1.0.604 (R2013a). Natick, Massachusetts: The MathWorks Inc.; 2013.

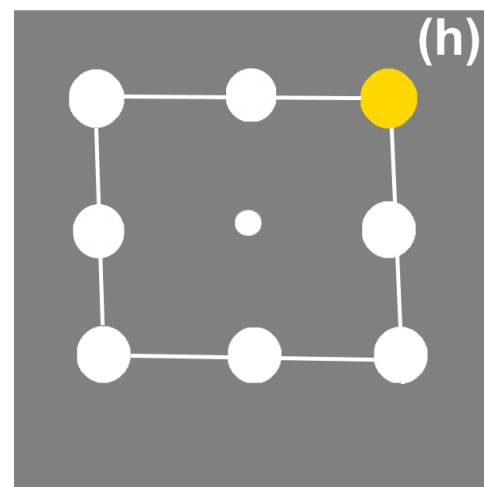
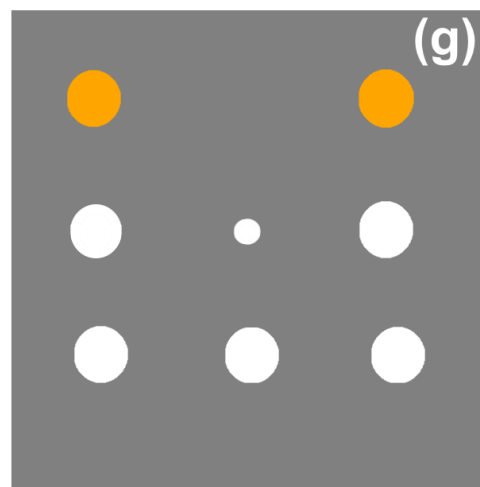
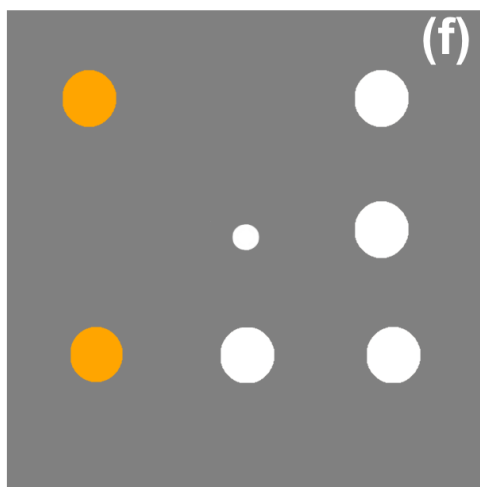
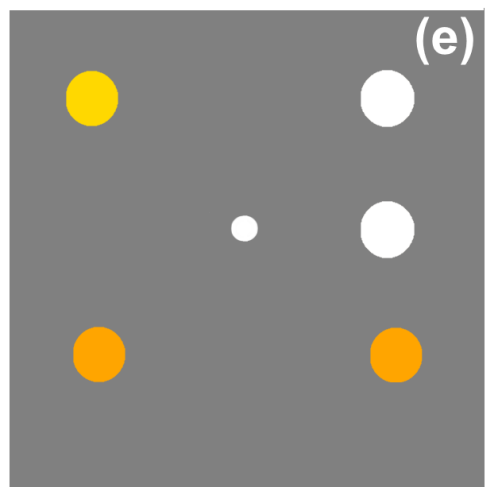
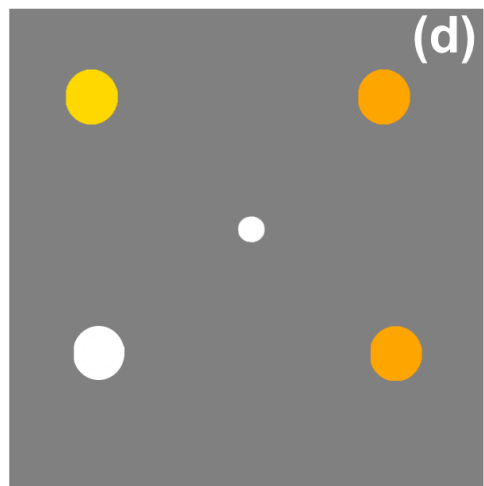
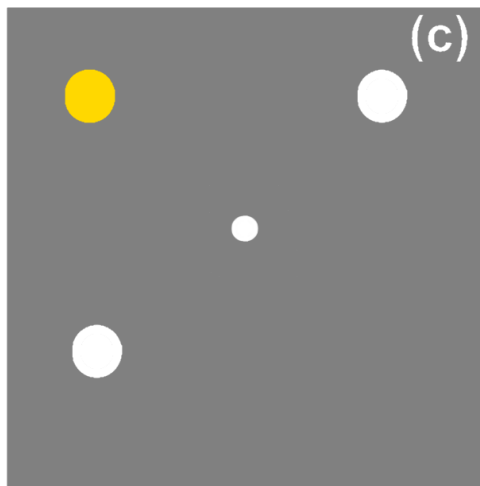
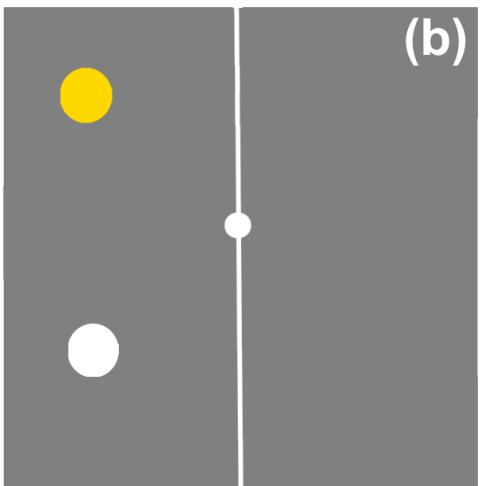
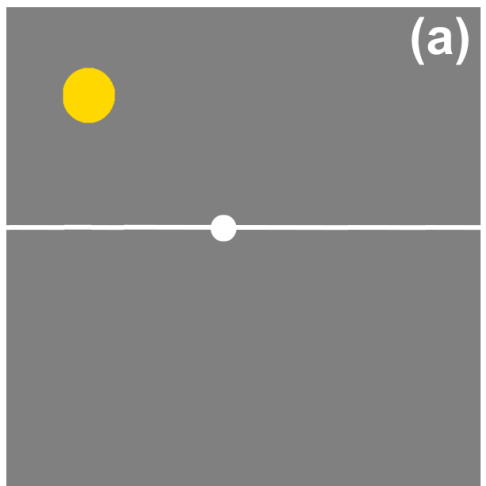
338 33. Brainard DH. The Psychophysics Toolbox. *Spatial Vision*. 1997;10(4):433-6.

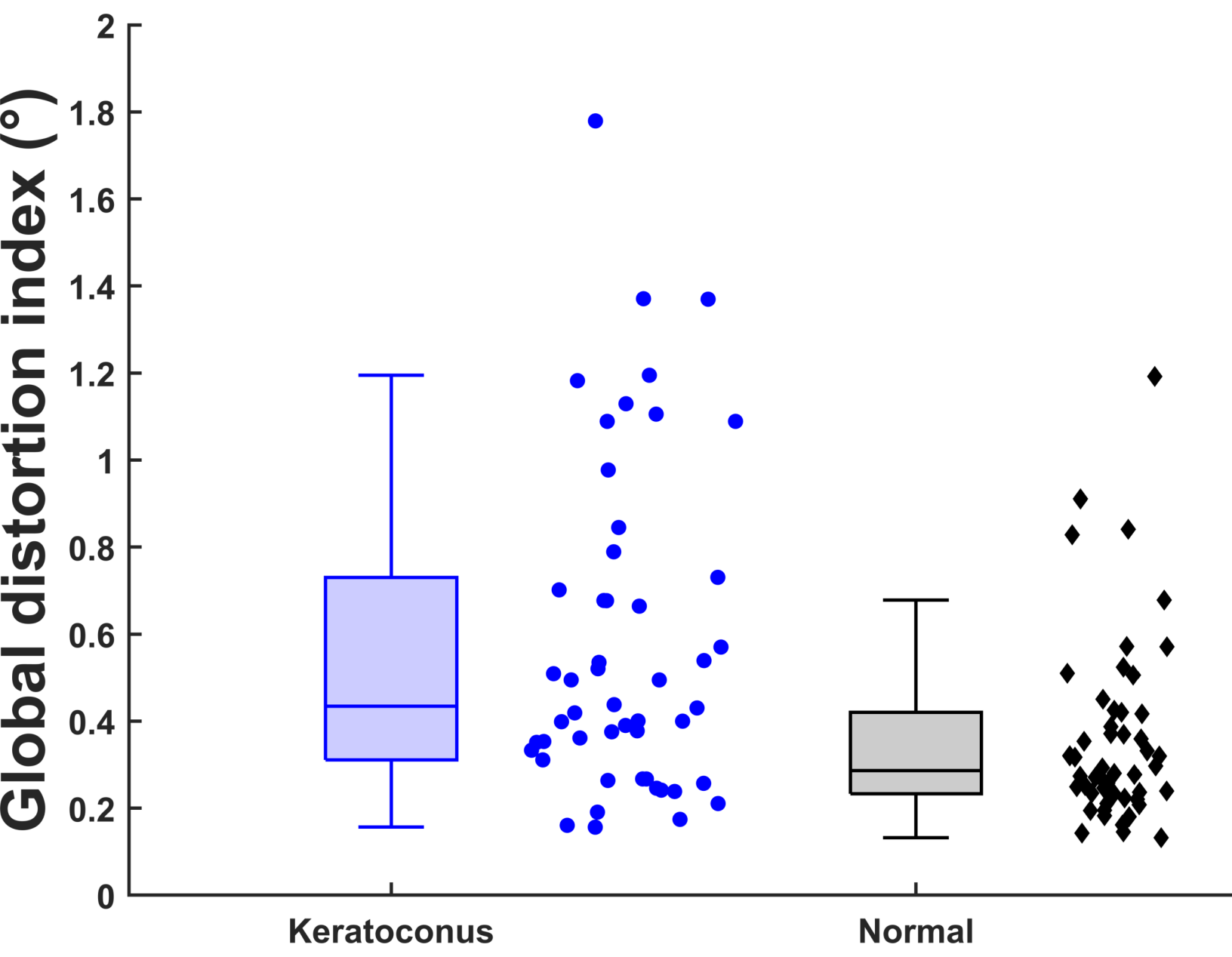
339 34. Kleiner M, Brainard D, Pelli D, Ingling A, Murray R, Broussard C. What's new in Psychtoolbox-
340 3? *Perception*. 2007;36:1-16.

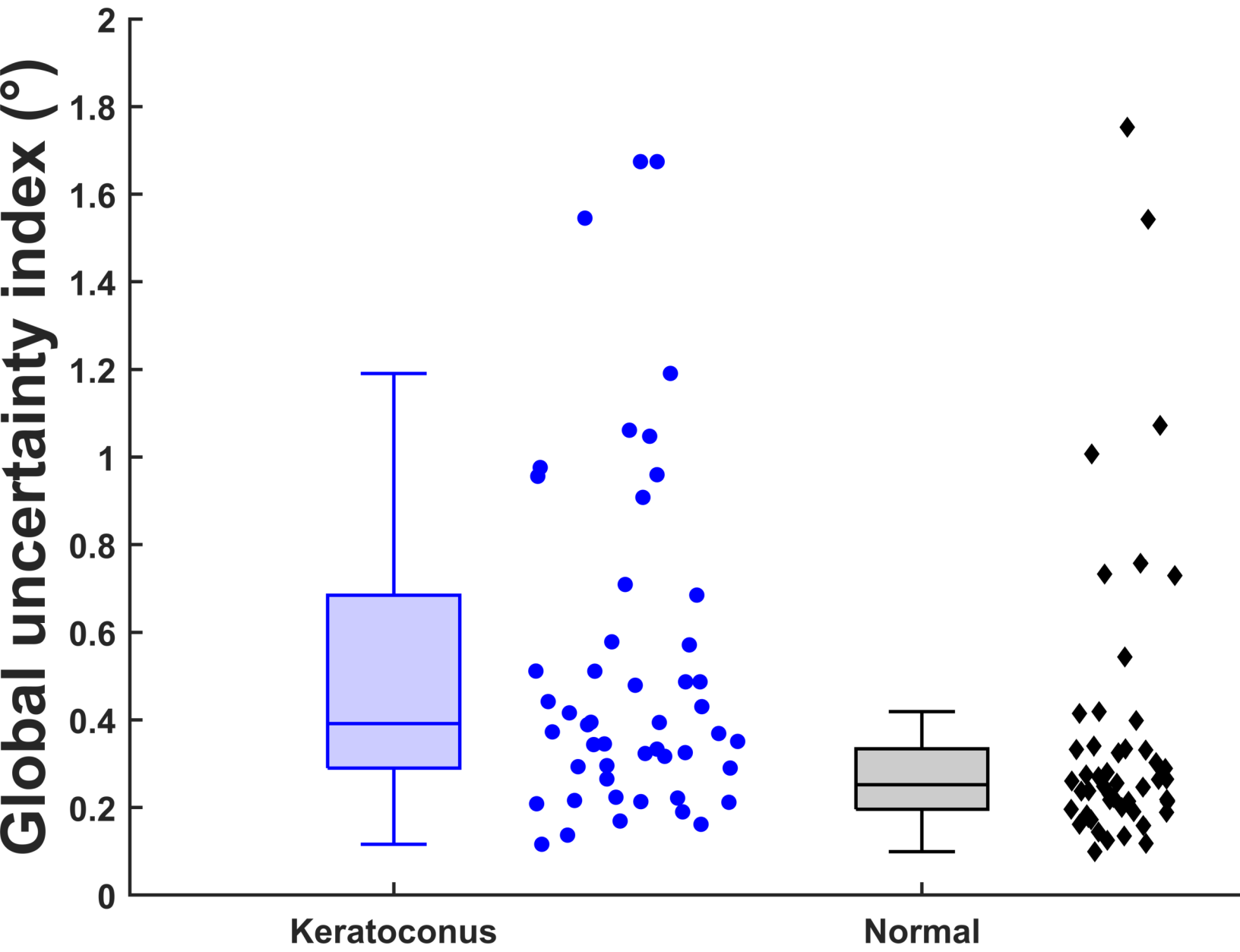
341 35. Piano MEF, Bex PJ, Simmers AJ. Perceived Visual Distortions in Juvenile Amblyopes
342 During/Following Routine Amblyopia Treatment. *Invest Ophthalmol Vis Sci*. 2016;57(10):4045-54.

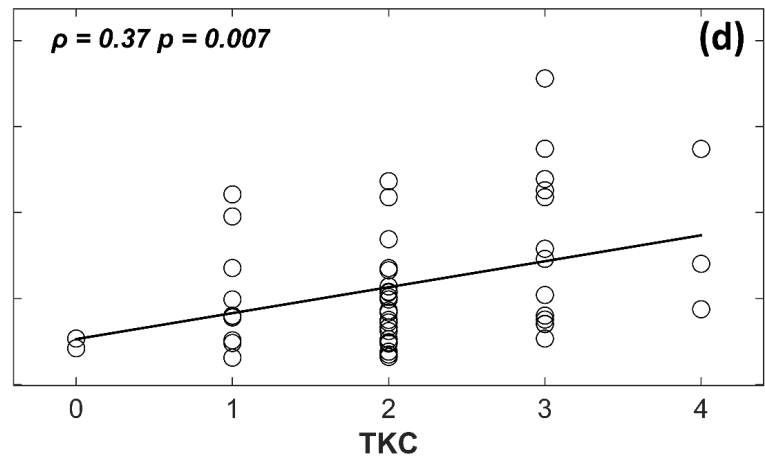
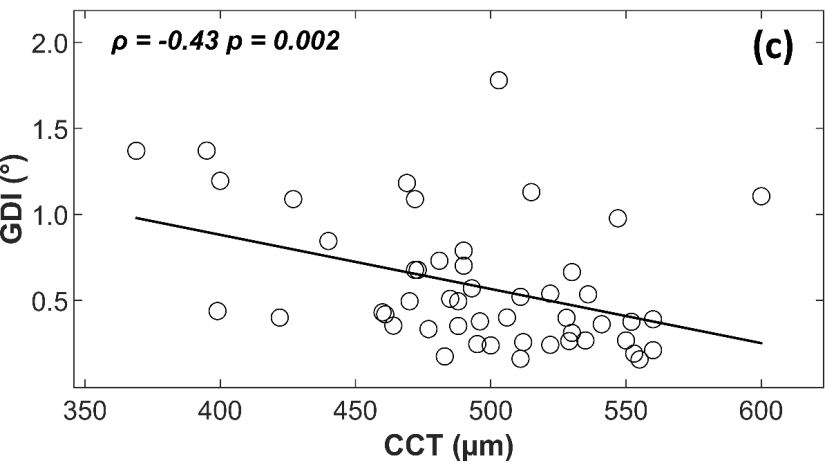
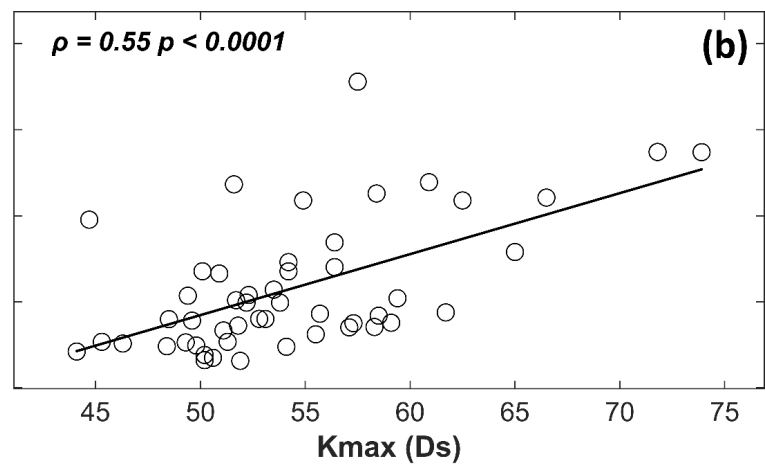
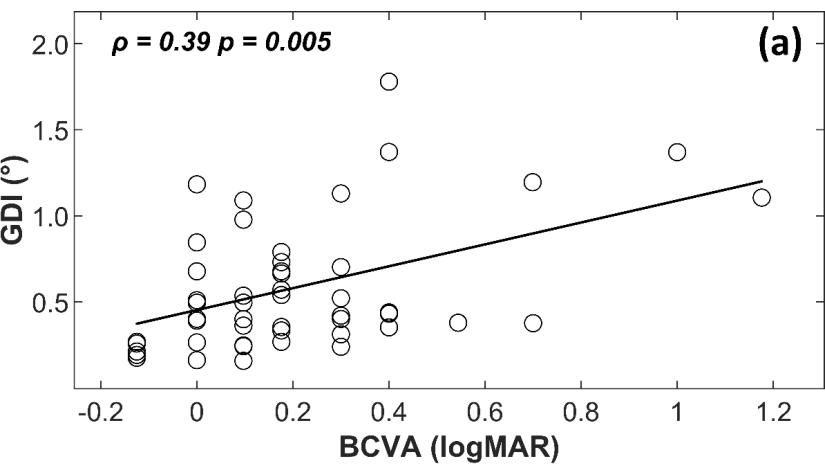
- 343 36. Loewenstein A, Malach R, Goldstein M, Leibovitch I, Barak A, Baruch E, et al. Replacing the
344 Amsler grid: A new method for monitoring patients with age-related macular degeneration11Drs.
345 Loewenstein, Malach, Alster, and Rafael: acknowledge a financial interest in Notal Vision.
346 Ophthalmology. 2003;110(5):966-70.
- 347 37. Liduma S, Luguzis A, Krumina G. The impact of irregular corneal shape parameters on visual
348 acuity and contrast sensitivity. BMC Ophthalmology. 2020;20(1):466.
- 349 38. Kymes SM, Walline JJ, Zadnik K, Sterling J, Gordon MO. Changes in the Quality-of-Life of
350 People with Keratoconus. American Journal of Ophthalmology. 2008;145(4):611-7.e1.
- 351 39. Saunier V, Mercier A-E, Gaboriau T, Malet F, Colin J, Fournié P, et al. Vision-related quality of
352 life and dependency in French keratoconus patients: Impact study. Journal of Cataract & Refractive
353 Surgery. 2017;43(12):1582-90.
- 354 40. Ward E, Wickens RA, O'Connell A, Culliford LA, Rogers CA, Gidman EA, et al. Monitoring for
355 neovascular age-related macular degeneration (AMD) reactivation at home: the MONARCH study.
356 Eye. 2021;35(2):592-600.
- 357 41. Che Hamzah J, Daka Q, Azuara-Blanco A. Home monitoring for glaucoma. Eye.
358 2020;34(1):155-60.
- 359 42. Aboobakar IF, Friedman DS. Home Monitoring for Glaucoma: Current Applications and
360 Future Directions. Seminars in Ophthalmology. 2021;36(4):310-4.
- 361 43. Jones PR, Campbell P, Callaghan T, Jones L, Asfaw DS, Edgar DF, et al. Glaucoma Home
362 Monitoring Using a Tablet-Based Visual Field Test (Eyecatcher): An Assessment of Accuracy and
363 Adherence Over 6 Months. American Journal of Ophthalmology. 2021;223:42-52.
- 364 44. Chaikitmongkol V. Home Monitoring for Age-Related Macular Degeneration. In: Chhablani J,
365 editor. Choroidal Neovascularization. Singapore: Springer Singapore; 2020. p. 363-73.

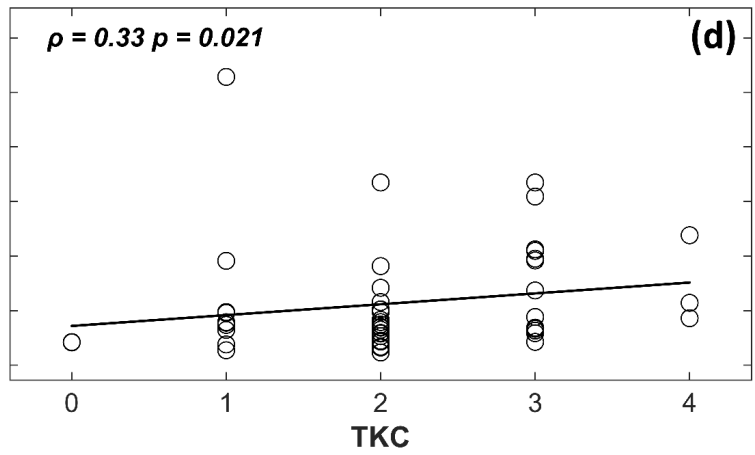
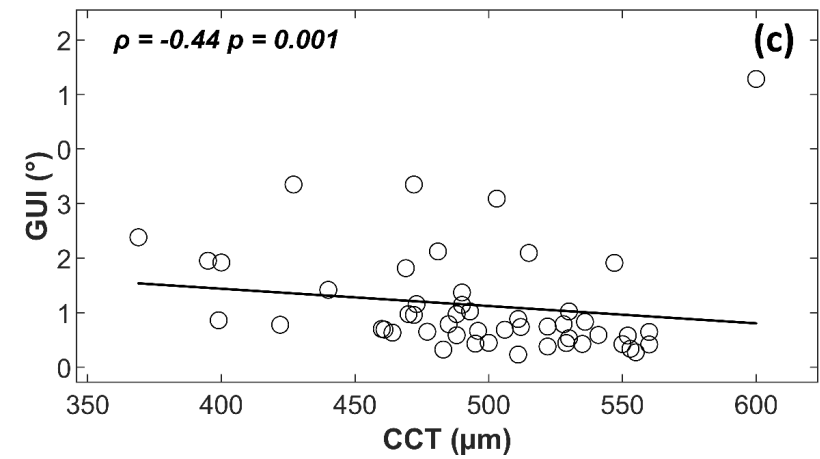
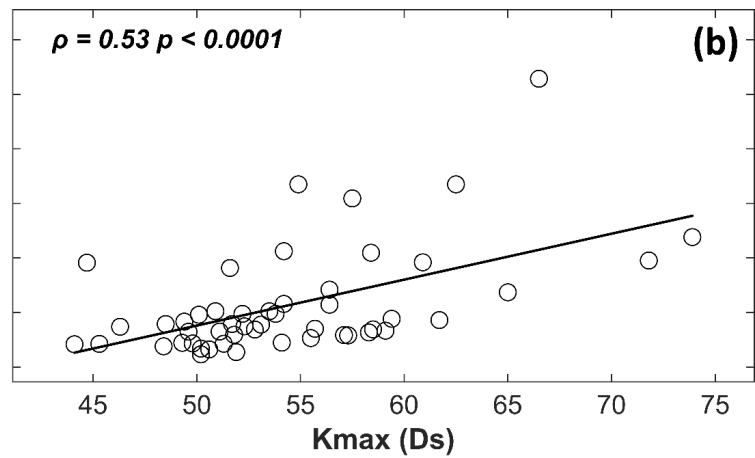
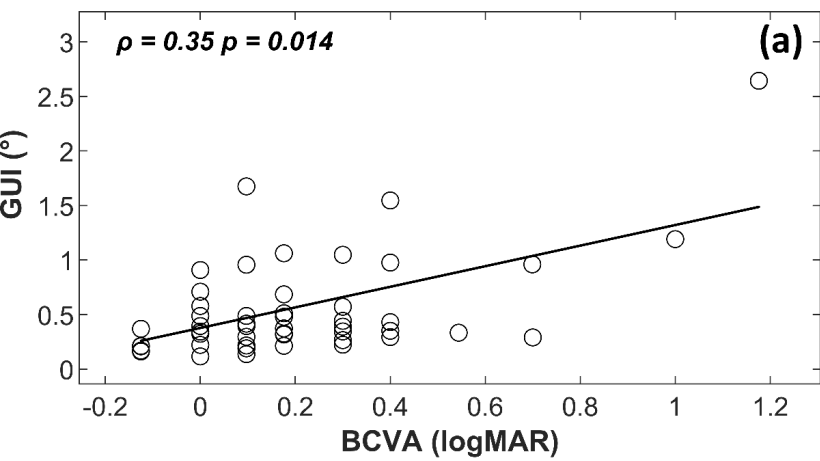
366











Clinical parameters	Keratoconus (<i>n</i> = 50 eyes)
Best-corrected visual acuity, log MAR, mean (SD)	0.21 (0.27)
Refractive error (Sphere), diopter cylinder, mean (SD)	- 2.52 (2.85)
Refractive error (Cylindrical), diopter cylinder, mean (SD)	-3.45 (2.10)
Maximum corneal curvature, dioptre, mean (SD)	54.48 (6.09)
Mean corneal curvature, dioptre, mean (SD)	47.03 (3.96)
Central corneal thickness, micrometre (μm), mean (SD)	495.34 (47.50)

Control ($n = 50$ eyes)

-0.09 (0.06)

- 1.14 (1.61)

-0.77 (0.90)

45.66 (1.58)

44.51 (1.41)

554.36 (25.71)
